An ultracold electron source as an injector for a compact SASE-FEL

An ultracold electron source as an injector for a compact SASE-FEL

2014 J. Phys. B: At. Mol. Opt. Phys. 47 234009

(http://iopscience.iop.org/0953-4075/47/23/234009)

IOP Publishing Journal of Physics B: Atomic, Molecular and Optical Physics
J. Phys. B: At. Mol. Opt. Phys. **47** (2014) 234009 (8pp) doi:10.1088/0953-4075/47/23/234009

An ultracold electron source as an injector for a compact SASE-FEL

S B van der Geer, E J D Vredenbregt, O J Luiten and M J de Loos

Department of Applied Physics, Eindhoven University of Technology, P O Box 513, 5600 MB Eindhoven, The Netherlands

E-mail: bas@pulsar.nl

Received 16 June 2014, revised 8 August 2014
Accepted for publication 14 August 2014
Published 24 November 2014

Abstract

Ultracold electron sources based on near-threshold photoionization of laser-cooled atomic gases can produce ultrashort electron pulses with a brightness potentially exceeding conventional pulsed electron sources. They are presently being developed for single shot ultrafast electron diffraction, where a bunch charge of 100 fC is sufficient. For application as an injector for x-ray free electron lasers (FEL) a larger bunch charge is generally required. Here we present preliminary calculations of an ultracold electron source operating at bunch charges up to 1 pC. We discuss the relevant bunch degradation processes that occur when the charge is increased. Using general particle tracer tracking simulations we show that bunches can be produced of sufficient quality for driving a 1 Å self amplified spontaneous emission free electron laser (SASE-FEL) at 1.3 GeV electron energy. In addition we speculate on the possibility of using the ultracold source for driving a 15 MeV SASE-FEL in Compton backscatter configuration into the quantum FEL regime.

Keywords: ultracold electron source, SASE-FEL, quantum FEL, particle tracking simulations

(Some figures may appear in colour only in the online journal)

1. Introduction

Ultra-short high-brightness electron bunches in the 30 keV–4 MeV energy range can be used for ultrafast electron diffraction (UED) experiments to study structural dynamics at atomic length and time scales [1]. Alternatively, they can be further accelerated to produce intense pulses of short-wavelength radiation by Compton backscattering [2], or they can be accelerated to GeV energies and fed into a self amplified spontaneous emission free electron laser (SASE-FEL) to produce ultra-short coherent x-ray pulses [3–5].

Each application puts its own particular demands on bunch quality, which can be expressed in terms of bunch charge, bunch length, energy spread and the transverse normalized root-mean-squared (rms) emittance $\epsilon_\perp$. The transverse normalized rms emittance is a Lorentz-invariant quantity, i.e. independent of beam energy U, which is given by

$$\epsilon_\perp = \frac{1}{mc}\sqrt{< x^2 >< p_x^2 > - < xp_x >^2}, \qquad (1)$$

where m and p are the electron mass and momentum, respectively, x is one of the transverse coordinates, k is Boltzmann's constant, c is the speed of light, and $<>$ indicates averaging over the bunch distribution. In a beam waist $<x\, p_x>$ vanishes so that

$$\epsilon_{\perp,\mathrm{waist}} = \sigma_x \frac{kT}{mc^2}, \qquad (2)$$

with σ_x the rms beam size and $T \equiv < p_x^2 > / (m\, k)$ the effective electron temperature associated with the transverse momentum distribution. For all applications the transverse emittance should preferably be as small as possible. This can be achieved by either minimizing the initial source size or the electron temperature of the source. For high bunch charges the minimal source size is limited by the available extraction fields, which only leaves reduction of the electron temperature of the source.

The bunch length and energy spread are related through the longitudinal normalized rms emittance $\epsilon_\parallel$, a Lorentz-

invariant quantity which is defined analogously:

$$\epsilon_{\parallel} = \frac{1}{mc}\sqrt{< z^2 >< p_z^2 > - < z\, p_z >^2}, \tag{3}$$

with z the longitudinal coordinate. For a bunch without energy chirp, i.e. in a 'longitudinal beam waist' ($< z\, p_z > = 0$), equation (3) reduces to

$$\epsilon_{\parallel \mathrm{waist}} = \frac{1}{mc}\sigma_z\, \sigma_{p_z} = \frac{1}{mc}\sigma_t\, \sigma_U, \tag{4}$$

with σ_t the rms bunch duration and σ_U the rms longitudinal energy spread. Like the transverse emittance, the longitudinal emittance can be expressed in units of length, but often the prefactor $1/mc$ in equation (4) is left out, in which case the longitudinal emittance is expressed in a product of time and energy. For applications such as UED and SASE-FEL a bunch duration in the order of 100 fs is required, which can only be achieved for high bunch charges if some form of bunch compression is applied (e.g., [6]). Due to conservation of longitudinal emittance (equation (4)) this goes at the expense of energy spread. If a small energy spread is required, then it becomes important to minimize the longitudinal emittance of the source as well.

The usual method for the production of ultrashort high-brightness electron bunches is photoemission by an ultrashort laser pulse from a flat cathode, which is characterized by an effective electron temperature of, typically, $T \approx 5000$ K ($kT \approx 0.5$ eV). State-of-the-art photoguns are able to produce bunches with a charge of $Ne = 100$ pC and a transverse normalized rms emittance $\epsilon_{\perp} = 0.5$ mm mrad from a spot with rms size $\sigma_x = 1$ mm. These devices have been fully optimized in the sense that their normalized brightness, expressed in terms of the transverse phase space density $N/\epsilon_{\perp}^2$, cannot be improved any further. This implies that the minimal transverse normalized emittance that can be achieved scales with the square root of bunch charge: $\epsilon_{\perp} \propto \sqrt{N}$.

An interesting new development is the ultracold electron source, which is based on near-threshold photoionization of laser-cooled atomic gases [7–15]. The ultracold source is characterized by effective temperatures as low as $T \sim 10$ K. This implies that for the same source size, and thus the same bunch charge, bunches can be produced with an emittance 1–2 orders of magnitude lower than by photoemission. In [11, 15] it was shown that even for femtosecond photoionization transverse source temperatures $\sim$10 K can be achieved. This surprising result seems to be in contradiction with the large bandwidth of the femtosecond photoionization laser pulses, which would suggest source temperatures at least an order of magnitude higher. A careful analysis of the photoionization process [11] has revealed that the excess kinetic energy imparted by the photon to the electron is generally not evenly distributed among the degrees of freedom. By a properly chosen combination of extraction electric field and ionization wavelength, the ensuing electron beam is squeezed in such a way that the transverse momentum spread is reduced at the expense of longitudinal energy spread.

Recently, the first electron diffraction patterns were obtained with picosecond bunches generated with the ultracold source [16]. In these experiments the amount of charge per bunch was limited to $N \leqslant 10^3$ to prevent beam degradation due to space charge effects. For single-shot UED experiments, however, $N \geqslant 10^6$ electrons per bunch are required to create a high quality diffraction pattern. In [17], we showed by charged particle tracking simulations that even without taking special measures to manage space charge effects, as have been developed for photocathode guns [18], the ultracold electron source is a promising candidate for single-shot UED experiments. In this paper we investigate the performance of the ultracold electron source in parameter regimes suitable to drive a compact SASE-FEL producing ultrashort coherent radiation pulses at hard x-ray wavelengths.

In a single pass free electron laser (FEL) it is essential that the emitted radiation overlaps the electron beam over a substantial distance. The electron and photon beams are properly matched if the betatron function of the electron beam is equal to or larger than the Rayleigh range of a diffraction limited photon beam. This condition can be expressed in terms of emittance and wavelength in the following way

$$\frac{\epsilon_{\perp}}{\beta\gamma} \leqslant \frac{\lambda}{4\pi}, \tag{5}$$

where λ is the wavelength of the produced radiation, $\beta \equiv v/c$, and $\gamma \equiv 1/\sqrt{1-\beta^2}$ the Lorentz factor, with v and c the velocity of the electrons and the speed of light, respectively.

Equation (5) shows that, in principle, a reduction of the transverse emittance would allow operation of a single pass SASE-FEL at lower beam energies, thus enabling a more compact device. Using the ultracold electron source as an injector would imply that the tens of GeV currently required for the Linac Coherent Light Source (LCLS) could be reduced by at least an order of magnitude. However, unlike the UED case, in a SASE-FEL a high peak current, and therefore a high bunch charge, is essential to enable sufficient gain for single pass FEL operation. In this paper we show that an ultracold electron source can be constructed that produces 1 pC bunches with 13 nm transverse slice emittance and 1 keV ps longitudinal emittance. The longitudinal emittance is sufficiently low to allow compression to 10 fs bunch length, corresponding to 100 A peak current. The combination of transverse emittance *and* peak current is sufficient to drive a small-scale SASE-FEL at 1.3 GeV, producing x-rays at a wavelength of 1 Å.

In all SASE-FEL s in operation today many photons are emitted per electron, so that quantum mechanical effects are negligible. It has been predicted that FEL may be operated in a quantum regime, in which far less than one photon is emitted per electron [19, 20]. This regime is entered when the longitudinal momentum spread of the electron beam is less than the momentum of the emitted photons. In that case the spectrum of the emitted radiation is not noisy, as in a classical SASE-FEL, but consists of a discrete number of individual spikes. In fact, in the extreme quantum case only a single transform-limited spike remains. Although predicted for years, the quantum regime has never been reached experimentally. One of the main obstacles is the lack of a suitable

electron source. Because the ultracold source not only provides the required low transverse emittance, but is, in principle, also capable of producing a very low longitudinal emittance, it is an interesting candidate.

The remainder of this paper is organized as follows: first a possible setup for an ultracold electron injector is presented which produces ∼100 keV electron bunches with very low longitudinal emittance. Then the physical processes are briefly discussed that are involved in the beam degradation of an ultracold high-brightness bunch. Subsequently, simulation results are presented showing the characteristics of the source under realistic conditions. Finally, the suitability of an ultracold source as injector for a SASE-FEL is discussed.

2. Set-up

The ultracold plasma (UCP) is a recent development in cold-atom physics [21]. UCPs can be created in compact setups by near-threshold ionization of a cloud of laser-cooled and trapped atoms, providing a unique medium with electron temperatures in the 10 K range [22], orders of magnitude lower than the 5000 K (0.5 eV) that is typical for photo-emission and field-emission sources.

The creation of a UCP is a two step process: first, an ultra-cold atom cloud is produced in a magneto-optical atom trap (MOT) by the radiation pressure of three orthogonal pairs of laser beams in combination with a quadrupole magnetic field produced by two coils in anti-Helmholtz configuration [23]. Subsequently, the trapped gas is ionized just above threshold using a two-photon ionization scheme. For rubidium this could be the combination of a 780 nm photon, exciting atoms to the $5P_{3/2}$ state, and a 480 nm photon, which ionizes the atoms in the $5P_{3/2}$ state. The advantage of this scheme, compared to single-photon ionization, is that the initial ionization volume can be tailored by adjusting the overlap of the excitation laser beam and the ionization laser beam. Such beam shaping is essential to manage space charge effects [14].

Typical MOTs contain between 10^8 and 10^{10} atoms, equivalent to tens to thousands of pC of charge when fully ionized. Using a Zeeman slower [23], the rate at which atoms are replenished can be a few 10^{10} atoms s^{-1} [24], so that extraction of 1 pC electron bunches at repetition rates greater than 1 kHz is possible in principle. Atomic densities are typically a few 10^{16} m^{-3} but 10^{18} m^{-3} can be reached with the dark-spot technique [25].

The setup which we investigate in this paper is specifically designed to produce short electron bunches at 100 keV with both low transverse emittance *and* low longitudinal emittance. The source consists of two stages: a dc initial acceleration section for extracting the electron bunch from the UCP and an rf acceleration cavity for boosting the bunch energy to ∼100 keV. The dc field in the initial acceleration section is generated by a pair of parallel electrodes. A 3 GHz pillbox cavity in TM_{010} mode, adjacent to the dc accelerator, provides the rf accelerating field. In figure 1 the dc–rf accelerator setup is schematically illustrated. The solid line in

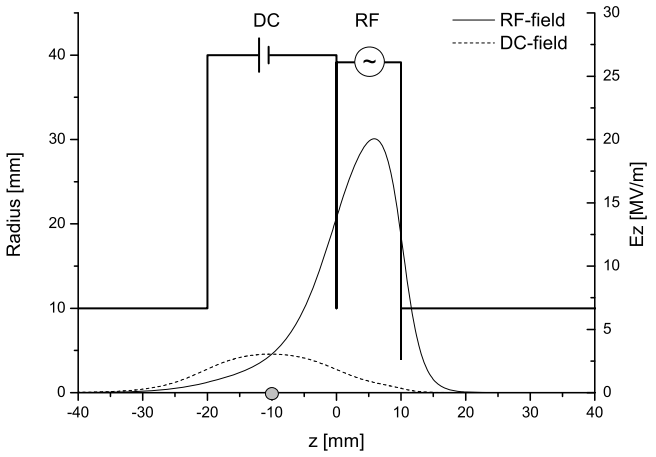

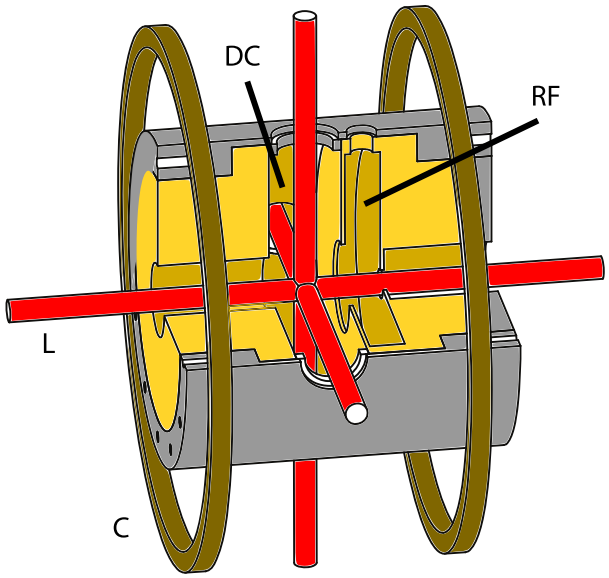

Figure 1. Schematic (top) and artistic (bottom) view of the geometry. The MOT traps the particles on-axis at $z = -10$ mm. This is inside a dc-field, and inside the tail field of the downstream rf-cavity. The trapped atoms are ionized at the moment that sum of these fields is zero, and subsequently accelerated in the downstream rf-cavity to 120 keV. L: ionization and trapping lasers; C: magnetic field coils; dc: dc acceleration section; rf: rf acceleration section.

the top figure indicates the actual inner dimensions of the different accelerator parts. The back plate of the pillbox at $z = 0$ mm also serves as ground plate for the dc accelerator.

The inside of the 3 GHz pillbox cavity extends from $z = 0$ to $z = 10$ mm. The maximum field amplitude of the rf field in the cavity is 20 MV m^{-1}. The cloud of ultracold atoms is trapped *outside* the cavity, at the position $z = -10$ mm. The amplitude of the tail field of the cavity at the position of the atom cloud is $E_0 = 3$ MV m^{-1}, as is shown in figure 1. The dc field also has a strength of $E_0 = 3$ MV m^{-1} at the position of the atom cloud. This creates a dc–rf electric field $E_z(t) = E_0(1 - \cos(\omega t))$ at the position of the atom cloud, where $\omega = 2\pi f$ with $f = 3$ GHz the resonant frequency. By ionizing the gas around the zero crossing at $t = 0$, a bunch is created in very low fields, thus minimizing the initial

longitudinal emittance. The iris of the cavity at $z = 0$ has a relatively large radius of 10 mm in order to create the required tail, while the downstream iris at $z = 10$ mm is kept small for more efficient acceleration.

3. Beam degradation mechanisms

Several processes may cause bunch quality degradation during the creation and acceleration of an ultracold bunch. The most fundamental mechanism is dilution of the phase space density by statistical Coulomb interactions between individual particles, also known as disorder induced heating. In addition, the phase space density distribution may get distorted during the process of extraction due to the interaction with the mean fields associated with the density distribution of the electrons and ions, the so-called space charge fields, and the interaction with the external acceleration fields. Such distortions of the phase space density distribution cause emittance growth both in the transverse and the longitudinal directions. Below estimates for the effects of these processes are briefly discussed. Based upon these estimates favorable operating parameters of the ultracold source are derived, which form the starting point for more detailed particle tracking simulations discussed in the next section.

3.1. Disorder induced heating

The random nature of the creation process causes excess potential energy that is converted to kinetic energy. This is known as disorder-induced heating. In a stationary ultra-cold plasma it will lead to a final temperature T_h of the order of the Coulomb interaction energy between neighboring electrons [26]

$$k\ T_\mathrm{h} \approx \frac{e^2}{4\pi\epsilon_0\ a}, \tag{6}$$

where $a = (4\pi\ n/3)^{-1/3}$ is the Wigner–Seitz radius, with n the electron number density, and where e and ϵ_0 are the elementary charge and vacuum permittivity respectively. This final temperature is reached on a timescale of the order of the inverse plasma frequency $\omega_p^{-1} = \sqrt{m\ \epsilon_0/n\ e^2}$. If we assume a MOT density $n = 10^{18}$ m^{-3} and full ionization in the volume defined by the overlap of the excitation and the ionization laser beams, a temperature $T_\mathrm{h} \approx 20$ K is reached within $\omega_p^{-1} \approx 20$ ps. During 20 ps electrons created in a field $E_0 = 3$ MV m^{-1} will travel a distance of only 100 μm, which is comparable to the typical size of the ionization volume. Since the time it takes to separate the electrons from the ions is comparable to the thermalization time, it is reasonable to assume that the initial distribution can be approximated by a thermal distribution with a temperature determined by the initial density, as given by equation (6).

In principle, the initial electron temperature of the plasma is also dependent on the bandwidth, and thus the duration, of the ionization laser pulse. The shorter the laser pulse duration Δt, the higher the initial temperature $\approx h/(k\ \Delta t)$, where h is Planck's constant and we assumed a Fourier transform limited pulse. The pulse duration $\Delta t \approx 1$ ps used in the simulations would therefore give rise to an initial temperatures of $\sim$10 K, approximately matched to the equilibrium temperature T_h. Furthermore, the momentum distribution immediately after ionization is not an isotropic Boltzmann distribution, but depends on the magnitude and the direction of the electric field vector and the direction of the polarization of the ionization laser pulse [11–13]. For the high bunch densities we are considering, however, the disorder-induced heating mechanism will remove any anisotropy and create a distribution that is close to thermal within tens of picoseconds. For detailed charged particle tracking simulations the starting point will therefore be a Boltzmann distribution with a temperature equal to the equilibrium temperature T_h of disorder-induced heating.

3.2. Longitudinal emittance growth during bunch creation

Due to the presence of an electric field, the first electrons created have moved to a different position in phase space at the moment the last atoms are ionized. The creation process thus fills a larger part of phase space than the phase-space volume of the initial particle coordinates. As a result, an electric field present during the creation process causes longitudinal phase space growth and hence bunch degradation. To estimate this effect, we present a simple model that assumes no correlations between the longitudinal position and longitudinal momentum coordinates.

Particles created at rest at time t_i have longitudinal momentum p_z at time t governed by the classical equations of motion: $p_z(t) = \int_{t_i}^{t} eE_z(t)\mathrm{d}t$. For simplicity we assume that t_i is uniformly distributed over the interval $[0, \Delta t]$, with Δt the ionization laser pulse duration. For a dc acceleration field $E_z = E_0$ we then find $\sigma_{p_z} = \frac{1}{\sqrt{3}} e\ E_0$, where σ_{p_z} is the rms value of p_z at $t = \Delta t$. Using the fact that the change in the rms length of the electron distribution σ_z during a time interval Δt can be neglected for typical values of σ_z, E_0, and Δt and that, by assumption, there is no correlation between position and momentum ($< z\ p_z > = 0$), we find that the rms normalized longitudinal emittance immediately after creation of the bunch is given by

$$\epsilon_{\parallel,\mathrm{dc}} = \frac{1}{mc}\sigma_z\ \sigma_{p_z} = \frac{1}{\sqrt{3}}\frac{e}{mc}\ E_0\ \sigma_z\ \Delta t. \tag{7}$$

For $E_0 = 3$ MV m^{-1}, $\Delta t = 1$ ps, and $\sigma_z = 50\ \mu$m this results in a longitudinal emittance $\epsilon_\parallel \approx 50$ nm or, equivalently, $\epsilon_\parallel \cdot mc \approx 0.1$ keV $\cdot$ ps, which is a value that can also be achieved with conventional photocathode guns.

For the dc–rf acceleration geometry described in section 2 the acceleration field is given by $E_z(t) = E_0(1 - \cos(\omega t))$ resulting in $\sigma_{p_z} = \frac{1}{8\sqrt{7}} e\ E_0\ \omega^2\Delta t^3 + O(\Delta t^5)$. We thus find

$$\epsilon_{\parallel,\mathrm{dc-rf}} = \frac{1}{mc}\sigma_z\ \sigma_{p_z} = \frac{1}{8\sqrt{7}}\frac{e}{mc}\ E_0\ \sigma_z\ \omega^2\Delta t^3, \tag{8}$$

implying a reduction of the longitudinal emittance by a factor $\sim\omega^2\Delta t^2 \ll 1$ with respect to the dc acceleration

geometry. For $E_0 = 3$ MVm, $\Delta t = 1$ ps, and $\sigma_z = 50\ \mu$m this results in an extremely low longitudinal emittance $\epsilon_\parallel \approx 1.5$ pm, or $\epsilon_\parallel \cdot mc \approx 3$ eV $\cdot$ fs. This clearly illustrates the advantage of the dc–rf acceleration geometry. Note that $\epsilon_{\parallel,\mathrm{dc-rf}}$ scales with Δt^3, so that the advantage is quickly lost for longer ionization pulse lengths. In addition, timing jitter between the ionization pulse and the rf field must be kept to a fraction of Δt. For example, when $\Delta t = 1$ ps, the longitudinal emittance $\epsilon_\parallel$ increases by a factor of 2 when the timing is off by 250 fs. However, synchronization to within 100 fs is possible [27].

3.3. Transverse emittance growth during bunch creation

As long as the ion and electron distributions overlap, the ion background creates an electric field precisely opposite to the electric field created by the electrons, thus preventing space charge distortion of the bunch and the associated emittance growth. However, the acceleration field pulls the electron and ion distributions apart. As soon as a part of the electron bunch emerges from the ion cloud, it will expand rapidly, while the rest of the bunch is kept together, only to expand at a later time. This is a complicated dynamical process, governed by Coulomb interactions between two different three dimensional charge distributions of opposite sign. The resulting emittance growth can only be estimated reliably by detailed charged particle tracking simulations. It is however possible to estimate straightforwardly for what bunch charges and acceleration field strengths this effect becomes important.

This is analogous to the effects of image and space charge fields during photoionization in photocathode devices, which remain manageable if the external acceleration field is at least an order of magnitude stronger than the maximum image and space charge fields. Based on this analogy we can make an estimate for the maximum bunch charge that is allowed for a given acceleration field strength. If we assume, for simplicity, a uniform spherical charge distribution cut off at $r = r_\mathrm{m}$, then the maximum space charge field strength is given by:

$$E_\mathrm{sc} = \frac{r_\mathrm{m} ne}{3\epsilon_0}. \tag{9}$$

Since beam quality is affected when E_sc becomes a significant fraction of the external field E_z, it follows that the maximum bunch charge Ne that is allowed is given by

$$Ne = \frac{4}{3}\pi r_\mathrm{m}^3 ne \ll \frac{36\pi\epsilon_0^3 E_z^3}{n^2 e^2}. \tag{10}$$

For a number density $n = 10^{18}$ and $E_z \approx 1$ MV m^{-1} this limits the total charge to $Ne \sim 1$ pC. Of course, this is a very rough estimate. Detailed numerical simulations using the actual density distributions are essential to reach a proper understanding of the charge limits.

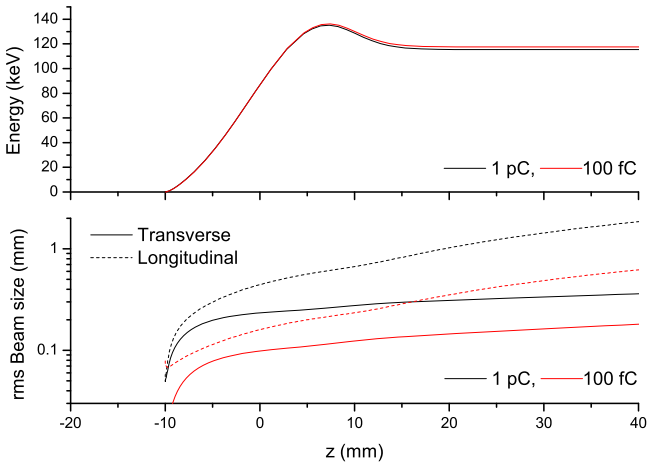

Figure 2. GPT simulations of bunch size and energy evolution as function of position for 1 pC (black) and 100 fC (red).

4. Simulation results

The proposed 1 pC ultracold electron source described in section 2 has been simulated with the general particle tracer (GPT) code [28]. This code tracks the relativistic equations of motion of sample particles through the combination of external fields and space charge fields. For the 1 pC case, space charge effects, including interaction between the ions and the electrons, are taken into account with an anisotropic particle-in-cell solver [29]. Disorder induced heating is accounted for by starting with an initial temperature $T = 10$ K.

Both the dc and the rf fields have been calculated with the SUPERFISH set of codes [30] on a $100 \times 100\ \mu$m and $150 \times 150\ \mu$m mesh respectively. Because the transverse dimension of the bunch is of the order of the mesh size, only the on-axis $E_z(z)$ profile is fed into the tracking code. The transverse dependence of the longitudinal electric field $E_z(z, r)$, the transverse electric field $E_r(z, r)$, and the azimuthal magnetic field $B_\phi(z, r)$ are derived from a Taylor expansion of the $E_z(z, r = 0)$ field [31]. In these simulations no other charged particle optics are used: the bunches are allowed to expand freely after acceleration.

The electrons are initiated sequentially in time, using a Gaussian temporal profile $\sim\exp(-t^2/2\sigma_t^2)$, with a FWHM duration of $2.355\ \sigma_t = 1$ ps. The initial velocity distribution is thermal with $\sigma_{v_x} = \sigma_{v_y} = \sigma_{v_z} = \sqrt{kT/m}$, with $T = 10$ K. The initial ionization volume, which is determined by the overlap between the excitation and ionization laser beams, is assumed to be a cylinder with a length L and radius R, with uniform density $n = 10^{18}$ m^{-3}. The 1 pC bunch ($N = 6.25 \times 10^6$) has an initial length equal to twice its radius R: $L = 2R$. For the given values of n and N it then follows that $L = 2R = 200\ \mu$m. The simulation results for the 100 fC bunch are based on an initial ionization volume with $L = 270\ \mu$m and $R = 27\ \mu$m [17]. All initial particle coordinates are chosen randomly in an uncorrelated way to correctly model the stochastic nature of the ionization process.

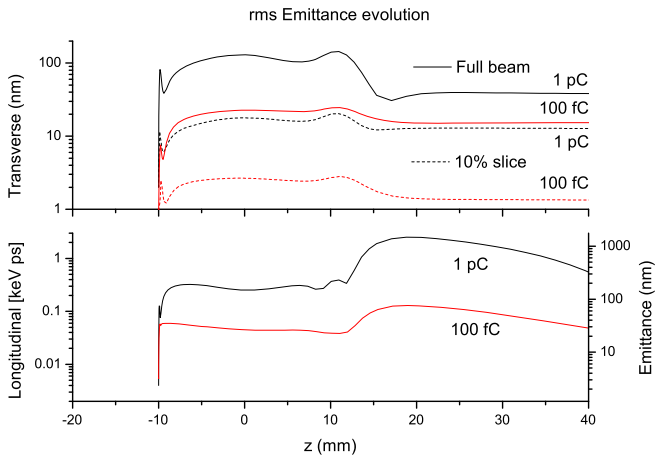

Figure 3. GPT simulations of emittance evolution as function of position for 1 pC (black) and 100 fC (red). The dashed lines are the emittance of the center 10% of the bunch.

Shown in figure 2 are GPT simulation results of a 1 pC bunch and a 100 fC bunch. The bunches are pulled into the rf-cavity, and subsequently accelerated to 120 keV. During this process, the bunch expands both longitudinally and transversely. The difference in longitudinal expansion speed between the 1 pC bunch and the 100 fC bunch clearly illustrates the strong space charge effects.

The main question is to what extent the quality of the bunch is degraded by the non-ideal external fields, space charge forces, and disorder induced heating. This is shown in figure 3 where the evolution of the longitudinal and transverse emittances is shown, taking into consideration all deteriorating effects mentioned above. The starting points of the evolution curves are determined by $T = 10$ K, as discussed in section 3. Both the transverse and longitudinal emittance increase sharply due to the extraction from the ion cloud. Interestingly, the emittance increases even more if we artificially remove the ion cloud from the GPT simulations. This is because the ions keep the electrons from moving to an other location in phase space during the ionization process. However, once the electrons and ions are pulled apart nonlinear forces between the two charged particle clouds come into play, which subsequently cause emittance degradation. The ions prevent emittance growth during ionization, when the ion and electron cloud still fully overlap, but are also the cause of emittance growth during the onset of acceleration. The latter process stops when the ion cloud and the electron cloud have become separated by a few bunch lengths.

The exit kick of the rf cavity at $z = 10$ mm has both transverse and longitudinal effects. In transverse phase-space it causes a slight realignment of the individual slices in transverse phase space, also known as emittance compensation [18], causing a small reduction in the projected transverse emitance. In longitudinal phase space it causes emittance growth. The external fields have not been optimized to reduce this effect.

The obtained transverse slice emittance is 13 nm for the 1 pC case and 1 nm for the 100 fC case. State-of-the-art rf photoguns produce bunches with 100 pC of charge with $\epsilon_\perp = 0.5\,\mu$m. Using the fact that for a given maximum brightness $\epsilon_\perp \propto \sqrt{N}$, this implies that optimized rf photoguns are capable of producing 1 pC bunches with a transverse emittance of 50 nm and 100 fC bunches with a transverse emittance of 15 nm. Consequently, the simulation results of the ultracold source are four times better in terms of transverse emittance compared to an rf photogun for 1 pC and over an order of magnitude better for the 100 fC case. Even better numbers seem possible, because it is likely that part of the emittance growth can be avoided by optimizing the initial density distribution [14] and by using specially designed external fields to undo space charge effects [18].

The obtained longitudinal emittance is of the order of 1 keV $\cdot$ ps for 1 pC bunches and 0.1 keV $\cdot$ ps for 100 fC bunches. These are respectable numbers, but the full potential of the dc–rf acceleration geometry has not been reached yet (see section 3.2). Clearly a lot is still to be gained by optimizing the initial volume and further design of the external fields.

5. Ultracold electron source as injector for a SASE-FEL

In a SASE-FEL, radiation is emitted with a resonance wavelength given by $\lambda = \lambda_u(1 + K^2/2)/(2\gamma^2)$, where λ_u is the undulator period, K a measure for the undulator strength and γ the Lorentz factor. The power of the emitted radiation grows proportional to $\exp(z/L_g)$, where the power gain length L_g can be approximated by

$$L_g = \frac{1}{\sqrt{3}}\left(\frac{2\,mc\gamma^3\sigma_x^2\lambda_u}{\mu_0 eK^2\hat{I}}\right)^{1/3}, \tag{11}$$

with σ_x the transverse beam size and $\hat{I}$ the peak current. Of particular importance in SASE-FEL theory is the FEL parameter ρ_{FEL} [32]. It is a measure for the number of undulator periods required per gain length, and consequently it is a measure for the relative bandwidth of the output spectrum. The FEL parameter is defined as

$$\rho_{FEL} = \frac{1}{4\pi\sqrt{3}}\frac{\lambda_u}{L_g}. \tag{12}$$

For a SASE-FEL it is essential that electrons emit their radiation in phase. Consequently, the relative energy spread σ_γ/γ must be below $\rho_{FEL}/2$. This sets a theoretical maximum to the peak current, limited by the longitudinal emittance ϵ_z, to

$$\hat{I} = \frac{Q}{e}\frac{\sigma_\gamma mc^2}{\epsilon_z}. \tag{13}$$

Furthermore, to have continuous overlap between the radiation and the electron bunch, the gain length L_g is not allowed to exceed the Rayleigh length $Z_R = 4\pi\sigma_x^2/\lambda$.

Given the above equations, we have all constraints in place to dimension a 1 Å SASE-FEL based on an ultracold electron source.

Table 1. Top: bunch parameters from GPT simulations of the presented ultracold electron source. Simulation results are described in this paper for the 1 pC case and identical to [17] for the 100 fC case. Bottom: settings for a SASE-FEL based on these sources.

		Classic	Quantum
Q	Charge	1 pC	100 fC
$\epsilon_\perp$	Slice emittance	13 nm	1 nm
ϵ_z	Longitudinal emittance	1 keV ps	0.1 keV ps
λ	Wavelength	1 Å	3.9 Å
$\gamma mc^2/e$	Energy	1.3 GeV	15 MeV
K	Undulator strength	0.1	0.5
$\hat{I}$	Peak current	100 A	1 mA
$\epsilon_\perp$	Maximum emittance	20 nm	1 nm
λ_u	Undulator period	1.3 mm	800 nm
L_g	Gain length	0.28 m	2 mm
ρ_{FEL}	FEL-parameter	0.0002	0.00002
P	Output power	25 MW	50 W
			60k photons
$\bar{\rho}$	Quantum FEL-parameter		0.1

Shown in the left-top part of table 1 is a summary of the bunch parameters of a 1 pC ultracold electron source as described above. The left-bottom part is a list of SASE-FEL parameters to produce narrow-band 1 Å radiation, based on a micro-undulator with $\lambda_u = 1$ mm. To reach the desired wavelength, acceleration to 1.3 GeV is required.

Construction of a 1 m long undulator with a period of 1 mm, four times smaller than the unulator presented in [33], is an obvious technical challenge that may well be solvable [34]. Also, emittance growth during acceleration must be kept to a minimum, and it is not immediately clear what may be possible here. In table 1, emittance is assumed to remain below 20 nm.

We note that the output power $P = \rho_{FEL}\,\hat{I}\,\gamma mc^2/e = 25$ MW is significantly less than the GW level reached by LCLS, primarily due to the lower charge. Operation at kHz repetition rate may be possible, given source parameters mentioned in section 2.

5.1. Quantum regime

Quantum effects in FELs are expected when the longitudinal electron momentum spread σ_{p_z} is less than the momentum $\hbar k$ of the emitted photon [19, 20]. It has been predicted that 'quantum purification' of the output spectrum should then occur, where in the extreme case only a single spike remains. A quantum FEL can be characterized by the dimensionless FEL parameter $\bar{\rho}$ given by:

$$\bar{\rho} = \frac{\sigma_p}{\hbar k} = \rho_{FEL}\frac{mc\gamma}{\hbar k}, \tag{14}$$

where quantum behavior occurs when $\bar{\rho} < 1$.

To reach this quantum regime, a high recoil momentum is obviously beneficial because it allows a larger energy spread. This however sets conflicting requirements for the acceleration energy. On the one hand, hard x-rays require a large acceleration energy to match the diffraction limited photon beam, see equation (5). On the other hand, a small acceleration energy is required to get a small $\bar{\rho}$, see equation (14). The solution to this problem is to start with an extremely small transverse emittance, as can be produced by an ultracold electron source. Furthermore, an extremely low longitudinal emittance is required to achieve low energy spread combined with the ability to compress to sufficient current. So far the quantum regime has never been observed experimentally. One of the reasons has been the lack of an electron source thats meets the above requirements. We suggest that the ultracold source is a potential candidate.

The right column in table 1 list experimentally attainable parameters to construct a SASE-FEL in the quantum regime and based on an ultracold electron source. The charge has been set to 100 fC, and the values for the transverse and longitudinal emittance are obtained from detailed GPT calculations presented in [17]. The static undulator is replaced by a high-power Ti : Sapphire laser in order to get the required short wavelength (high recoil momentum) at low energy. Essentially the experiment is Compton backscattering of a low-energy-spread electron beam by a counter propagating high-power 800 nm laser pulse. The remainder of the parameters listed in the table follow from direct application of equations (5), (11), (12), (13), and (14).

From $\bar{\rho} = 0.1$ we see that an ultracold electron source may indeed have the quality to act as an injector for a SASE-FEL in the quantum regime. We realize that the required high power laser undulator constitutes an interesting challenge as well: the combination of $K = 0.5$ and $\lambda_u = 800$ nm can be translated into a laser intensity of $I \approx 5 \times 10^{21}$ W m^{-2}. If we assume a Rayleigh range equal to the gain length, i.e. $L_g = Z_R = 2\pi w_0^2/\lambda_u$, then the laser beam waist $w_0 = 15\ \mu$m and the required peak laser power $P = 4$ TW. Since the electron bunch has to interact with the laser field over the entire Rayleigh range, the laser pulse length should be equal to at least the Rayleigh range, resulting in a laser pulse energy of $E \approx 30$ J. These laser beam parameters are well within the range of commercially available technology. To reach full saturation, however, typically 15 gain lengths are required, implying $Z_R = 15L_g$. Since both the required peak laser power P and the laser pulse length are proportional to the Rayleigh range, the required laser pulse energy $E \propto Z_R^2$, resulting in ~6 kJ, ~100 ps laser pulses. This is somewhat more challenging but still conceivable.

6. Conclusion

Ultracold electron sources can produce electron bunches with substantially lower emittance than rf photoguns. They are therefore promising sources for compact SASE-FELs, because every decrease in emittance of the source translates into an equal decrease in required energy. GPT tracking results show that a 1 pC ultracold electron source produces sufficient beam quality to drive a 1.3 GeV SASE-FEL at 1

Å wavelength. By optimizing the initial density distribution and using specially designed external fields, space charge effects may be reduced, which would lead to even better performance. This is the subject of further investigation.

In a low-charge, low-energy regime and in a Compton backscattering configuration, we speculate that an ultracold electron source may have sufficient quality to act as an injector for a SASE-FEL in the quantum regime. This intriguing possibility deserves further study as well.

Acknowledgements

We would like to thank R Bonifacio for fruitful discussions and motivating comments.

References

[1] Sciaini G and Miller R J D 2011 Femtosecond electron diffraction: heralding the era of atomically resolved dynamics *Rep. Prog. Phys.* **74** 096101
[2] Schoenlein R W, Leemans W P, Chin A H, Volfbeyn P, Glover T E, Balling P, Zolotorev M, Kim K-J, Chattopadhyay S and Shank C V 1996 Femtosecond x-ray pulses at 0.4 Å generated by 90° Thomson scattering: a tool for probing the structural dynamics of materials *Science* **274** 236
[3] Emma P *et al* 2010 First lasing and operation of an Ångstrom-wavelength free electron laser *Nat. Photonics* **4** 641
[4] Ackermann W *et al* 2007 Operation of a free-electron laser from the extreme ultraviolet to the water window *Nat. Photonics* **1** 336
[5] Tanaka H, Yabashi M *et al* 2012 A compact X-ray free-electron laser emitting in the sub-Ångström region *Nat. Photonics* **6** 540
[6] van Oudheusden T, de Jong E F, van der Geer S B, Op't Root W P E M, Luiten O J and Siwick B J 2007 Electron source concept for single-shot sub-100 fs electron diffraction in the 100 keV range *J. Appl. Phys.* **102** 093501
[7] Claessens B J, van der Geer S B, Taban G, Vredenbregt E J D and Luiten O J 2005 Ultracold electron source *Phys. Rev. Lett.* **95** 164801
[8] Claessens B J, Reijnders M P, Taban G, Luiten O J and Vredenbregt E J D 2007 Cold electron and ion beams generated from trapped atoms *Phys. Plasmas* **14** 093101
[9] Taban G, Reijnders M P, Bell S C, van der Geer S B, Luiten O J and Vredenbregt E J D 2008 Design and validation of an accelerator for an ultracold electron source *Phys. Rev. ST Accel. Beams* **11** 050102
[10] Taban G, Reijnders M P, Fleskens B, van der Geer S B, Luiten O J and Vredenbregt E J D 2010 Ultracold electron source for single-shot diffraction studies *Europhys. Lett.* **91** 46004
[11] Engelen W J, van der Heijden M A, Bakker D J, Vredenbregt E J D and Luiten O J 2013 High-coherence electron bunches produced by femtosecond photoionization *Nat. Commun.* **4** 1693
[12] Engelen W J, Smakman E, Bakker D J, Luiten O J and Vredenbregt E J D 2014 Effective temperature of an ultracold electron source based on near-threshold photoionization *Ultramicroscopy* **136** 73
[13] Engelen W J, Bakker D J, Luiten O J and Vredenbregt E J D 2013 Polarization effects on the effective temperature of an ultracold electron source *New. J. Phys.* **15** 123015
[14] McCulloch A J, Sheludko D V, Saliba S D, Bell S C, Junker M, Nugent K A and Scholten R E 2011 Arbitrarily shaped high-coherence electron bunches from cold atoms *Nat. Phys.* **7** 785
[15] McCulloch A J, Sheludko D V, Junker M and Scholten R E 2013 High-coherence picosecond electron bunches from cold atoms *Nat. Commun.* **4** 1692
[16] van Mourik M W, Engelen W J, Vredenbregt E J D and Luiten O J 2014 Ultrafast electron diffraction using an ultracold source *Struct. Dyn.* **1** 034302
[17] van der Geer S B, de Loos M J, Vredenbregt E J D and Luiten O J 2009 Ultracold electron source for single-shot, ultrafast electron diffraction *Microsc. Microanal.* **15** 282
[18] Serafini L and Rosenzweig J B 1997 Envelope analysis of intense relativistic quasilaminar beams in rf photoinjectors: a theory of emittance compensation *Phys. Rev.* E **55** 7565
[19] Bonifacio R, Piovella N and Robb G R M 2005 Quantum theory of SASE FEL *Nucl. Instrum. Methods Phys. Res.* A **543** 645
[20] Bonifacio R, Piovella N, Cola M M, Volpe L, Schiavi A and Robb G R M 2008 The quantum free-electron laser *Nucl. Instrum. Methods Phys. Res.* A **593** 69
[21] Killian T C, Kulin S, Bergeson S D, Orozco L A, Orzel C and Rolston S L 1999 *Phys. Rev. Lett.* **83** 4776
For reviews, see Gallagher T F *et al* 2003 *J. Opt. Soc. Am.* B **20** 1091
Killian T C 2007 Ultracold neutral plasmas *Science* **316** 705
[22] Kuzmin S G and O'Neil T M 2002 *Phys. Rev. Lett.* **88** 065003
[23] Metcalf H and van der Straten P 1999 *Laser Cooling and Trapping* (New York: Springer)
[24] Streed E W, Chikkatur A P, Gustavson T L, Boyd M, Torii Y, Schneble D, Campbell G K, Pritchard D E and Ketterle W 2006 Large atom number Bose–Einstein condensate machines *Rev. Sci. Instrum.* **77** 023106
[25] Radwell N, Walker G and Franke-Arnold S 2013 Cold-atom densities of more than 10^{12} cm^{-3} in a holographically shaped dark spontaneous-force optical trap *Phys. Rev.* A **88** 043409
[26] Chen Y C, Simien C E, Laha S, Gupta P, Martinez Y N, Mickelson P G, Nagel S B and Killian T C 2004 Electron screening and kinetic energy oscillations in a strongly coupled plasma *Phys. Rev. Lett.* **93** 265003
[27] Brussaard G J H, Lassise A, Pasmans P L E M, Mutsaers P H A, van der Wiel M J and Luiten O J 2013 Direct measurement of synchronization between femtosecond laser pulses and a 3 GHz radio frequency electric field inside a resonant cavity *Appl. Phys. Lett.* **103** 141105
[28] www.pulsar.nl/gpt
[29] Pöplau G, van Rienen U, van der Geer B and de Loos M 2004 Multigrid algorithms for the fast calculation of space-charge effects in accelerator design *IEEE Trans. Magn.* **40** 714
[30] Billen J H and Young L M Poisson superfish *Los Alamos National Laboratory Report* No. LA-UR-96-1834
[31] Jiye X 1986 *Aberration Theory in Electron and Ion Optics* (New York: Academic) p 18
[32] Bonifacio R, Pellegrini C and Narducci L M 1984 Collective instabilities and high-gain regime in a free electron laser *Opt. Commun.* **50** 373
[33] Paulson K P 1990 Micro-undulator research at UCSB *Nucl. Inst. Methods Phys. Res.* A **296** 624
[34] Harrison J, Joshi A, Lake J, Candler R and Musumeci P 2012 Surface-micromachined magnetic undulator with period length between 10 μm and 1 mm for advanced light sources *Phys. Rev. ST Accel. Beams* **15** 070703